Antiviral Research 100 (2013) 460–472

Contents lists available at ScienceDirect

Antiviral Research

journal homepage: www.elsevier.com/locate/antiviral

Inhibition of influenza virus internalization by (−)-epigallocatechin-3-gallate

Meehyein Kim [a,*], So-Yeon Kim [a], Hye Won Lee [a], Jin Soo Shin [a], Pilho Kim [b], Young-Sik Jung [b], Hyeong-Seop Jeong [c], Jae-Kyung Hyun [c], Chong-Kyo Lee [a]

[a] Virus Research and Testing Group, Korea Research Institute of Chemical Technology, Sinseongno, Yuseong, Daejeon 305-600, South Korea
[b] Cancer and Infectious Diseases Therapeutics Research Group, Korea Research Institute of Chemical Technology, Sinseongno, Yuseong, Daejeon 305-600, South Korea
[c] Division of Electron Microscopic Research, Korea Basic Science Institute, Gwahangno, Yuseong, Daejeon 305-333, South Korea

ARTICLE INFO

Article history:
Received 14 May 2013
Revised 19 July 2013
Accepted 3 August 2013
Available online 15 August 2013

Keywords:
Influenza virus
(−)-Epigallocatechin-3-gallate
Antiviral activity
Viral entry
Membrane damage

ABSTRACT

(−)-Epigallocatechin-3-gallate (EGCG), one of the major flavonoid components of green tea, is known to have a broad antiviral activity against several enveloped viruses, including the influenza virus. However, its mode of action and the mechanism that allows it to target influenza virus molecules have not been fully elucidated. Thus, this study investigated the molecular mechanism by which EGCG suppresses influenza virus infections. EGCG was found to block an early step in the influenza viral life cycle, but it did not affect viral adsorption to target cells or viral RNA replication. However, EGCG inhibited hemifusion events between virus particles and the cellular membrane by reducing the viral membrane integrity, thereby resulting in the loss of the cell penetration capacity of the influenza virus. EGCG also marginally suppressed the viral and nonviral neuraminidase (NA) activity in an enzyme-based assay system. In conclusion, it is suggested that the anti-influenza viral efficacy of EGCG is attributable to damage to the physical properties of the viral envelope and partial inhibition of the NA surface glycoprotein. These results may facilitate future investigations of the antiviral activity of EGCG against other enveloped viruses as well as influenza virus.

1. Introduction

At present, the regimens used to treat human influenza virus infections are based on viral neuraminidase (NA) inhibitors, such as oseltamivir (OSV), zanamivir, peramivir, and laninamivir, and viral matrix protein 2 (M2) inhibitors, including amantadine and rimantadine (De Clercq, 2006; McKimm-Breschkin, 2013). Drugs derived from sialic acid moieties that target NA protein are preferable to M2 inhibitors because of their high efficiency and stringent specificity, as well as their desirable safety profiles. However, the incidence of oseltamivir-resistant viruses is increasing, primarily because of the mutation of a single NA amino acid (H275Y according to the N1 numbering system or H274Y according to the N2 numbering system). This mutation has been reported in patients treated with oseltamivir but also in patients who have not received this drug (Hurt et al., 2012; van der Vries et al., 2010). The emergence of drug-resistant strains highlights the need to develop novel antiviral drugs that effectively target other viral proteins or cellular factors involved in the influenza virus life cycle, or the identification of novel NA inhibitors that do not recognize the same amino acids binding to the existing sialic acid derivatives.

(−)-Epigallocatechin-3-gallate (EGCG) is the major catechin found in green tea, which accounts for approximately 50% of the total catechins. This edible natural compound has demonstrable benefits, including antitumor, anti-oxidative, and antiviral effects (Cabrera et al., 2006; Yang et al., 2002). EGCG is multipotent in terms of its broad-spectrum antiviral efficacy *in vitro*, with inhibitory effects on human immunodeficiency virus (HIV) (Hauber et al., 2009; Kawai et al., 2003; Li et al., 2011), herpes simplex virus (HSV) (Isaacs et al., 2008; Lyu et al., 2005), hepatitis C virus (HCV) (Calland et al., 2012; Chen et al., 2012; Ciesek et al., 2011), and influenza virus (Nakayama et al., 1993; Song et al., 2005). Most studies of the mode of action of EGCG have shown that it blocks viral entry by inactivating the viral envelope proteins or cellular receptors, or it interferes with the activity of viral polymerase (Chen et al., 2012; Li et al., 2011). Its potential to inhibit influenza virus infections has been investigated extensively (Nakayama et al., 1993; Song et al., 2005, 2007). According to previous reports, EGCG can reduce the hemagglutinin (HA)-mediated hemolysis of chicken red blood cells (RBCs) and downregulate the endonuclease activity of the viral polymerase component PA, NA activity, and the dsRNA-binding ability of nonstructural protein 1 (NS1) (Cho et al., 2012; Kuzuhara et al., 2009; Song et al., 2005). Even though the potential anti-influenza virus effects of purified EGCG and its multiple inhibitory effects against several viral proteins have been reported,

* Corresponding author. Tel.: +82 42 860 7540; fax: +82 42 860 4246.
E-mail address: mkim@krict.re.kr (M. Kim).

0166-3542/$ - see front matter © 2013 Elsevier B.V. All rights reserved.
http://dx.doi.org/10.1016/j.antiviral.2013.08.002

its mode of action has not been fully elucidated by systematically tracing the viral replication steps it affects in cells.

The present study compared the antiviral activities of several monomeric and dimeric catechins using a cytopathic effect (CPE) reduction assay. EGCG had the most potent antiviral effect of the catechins tested in this study. It was found that EGCG inhibited the early steps in the viral replication cycle, where it did not affect influenza virus adsorption or its polymerase activity. In conclusion, EGCG blocked virus penetration into cells by physically damaging the viral integrity and it had marginal suppressive effects on the activity of NA. These findings may explain the general antiviral mechanism of EGCG against infections with influenza virus and possibly other enveloped viruses.

2. Materials and methods

2.1. Chemicals

The commercially available standard antiviral agents used in this study were amantadine hydrochloride (AMT) and ribavirin (RBV) obtained from Sigma (St Louis, MO), oseltamivir carboxylate (OSV-C) from US Biological (Swampscott, MA), and arbidol hydrochloride (ARB) from AK Scientific, Inc. (Mountain View, CA). Favipiravir (T-705; 6-flouro-3-hydroxy-2-pyrazinecarboxamide) was synthesized in-house by I.Y. Lee. The sulfated polysaccharide p-KG03, which was derived from the microalgae *Gyrodium impudium* (Yim et al., 2003), was purified by Yim at the Korea Polar Research Institute, South Korea. EGCG and other catechin derivatives, used in the CPE reduction assay, including epigallocatechin (EGC), epicatechin monogallate (ECG), and 2′2′-bisepigallocatechin digallate (bEGCdG), were obtained from a chemical library (The Spectrum Collection; MicroSource Discovery Systems, Inc., Gaylordsville, CT). The molecular weight and purity of EGCG (Sigma) used in the extended antiviral studies were characterized by liquid chromatography–mass spectrometry (LC–MS).

2.2. Cells and viruses

Madin-Darby canine kidney (MDCK) cells (ATCC, Manassas, VA) were grown in minimum essential medium (MEM; Gibco/Invitrogen, Carlsbad, CA) supplemented with 10% fetal bovine serum (FBS; Invitrogen) at 37 °C. Human embryonic kidney (HEK) 293T cells and African green monkey kidney Vero cells (ATCC) were grown at 37 °C in Dulbecco's Modified Eagle's Medium (DMEM; Gibco/Invitrogen) supplemented with 10% FBS (Invitrogen). Influenza virus strains A/Puerto Rico/8/34 (H1N1) (PR8) and A/Hong Kong/8/68 (H3N2) (HK) were obtained from ATCC and propagated in 10-day-old chicken embryos at 37 °C. Influenza virus A/Brisbane/59/2007 (H1N1) (BB) was obtained from the Center for Disease Control and Prevention (CDC, Atlanta, GA) *via* the Korea CDC at Cheongwon, South Korea, and A/Taiwan/1/1986 (H1N1) (TW), 2009 pandemic A/Korea/01/2009 (H1N1) (KR), and B/Panama/45/1990 (PNM) were obtained directly from the Korean CDC. These strains were propagated by infecting eggs at 37 °C (KR), or MDCK cells at 35 °C (BB) or 33 °C (TW and PNM), for 3 days.

2.3. Antiviral assay

In the CPE reduction assay, MDCK cells were seeded in 96-well plates and either mock-infected or infected with influenza virus at a multiplicity of infection (MOI) of 0.001 [50 plaque-forming units (PFU) of influenza virus per well]. After incubation for 1 h at 33 °C (mock, TW, and PNM) or 35 °C (PR8, BB, KR, and HK), the medium was removed, and test and standard chemicals were added, which were serially diluted in MEM containing 2 μg/ml TPCK-trypsin (Sigma). On day 2 or 3 post-infection (p.i.), the cell viability was measured after treatment with fluorescein diacetate (FDA; Sigma), as described previously (Kim et al., 2012; Schols et al., 1988). The 50% cytotoxic concentration (CC_{50}) and the 50% effective concentration (EC_{50}) values were calculated using SoftMax Pro Software (Molecular Devices, Sunnyvale, CA).

In the plaque inhibition assay, MDCK cells were seeded in 48-well plates and infected with influenza virus (MOI = 0.0005; 25 PFU/well) for 1 h at 33 °C or 35 °C. After washing with phosphate-buffered saline (PBS), the cell monolayers were overlaid with overlay medium [MEM containing 0.5% carboxymethylcellulose (CMC; Sigma) and 2 μg/ml of TPCK-trypsin (Sigma)] in the absence or presence of serially diluted chemicals. After incubation for 2 or 3 days, the viral plaques were visualized by staining with crystal violet. In the time of addition experiment, MDCK cells were infected with influenza virus PR8 at the same MOI at 4 °C for 1 h and the unadsorbed virus was removed. EGCG and a control compound (ARB) were added at 0, 1, 2, and 4 h p.i. At 5 h p.i., the cells were washed with PBS and overlaid with overlay medium.

2.4. Quantitative and semi-quantitative RT-PCR

The viral RNA was purified from the culture supernatants or ultracentrifugation fractions using a QIAamp Viral RNA kit (Qiagen, Hilden, Germany) and reverse transcribed to cDNA using SuperScript III reverse transcriptase (Invitrogen) and an influenza viral RNA-specific, universal primer (5′-AGCAAAAGCAGG-3′) (Hoffmann et al., 2001). Quantitative PCR was performed using PR8 NS-specific primers (NSfwd, 5′-CATAATGGATTCAAACACTGTGTC-3′; NSrev, 5′-CCTCTTAGGGATTTCTGATCTCGG-3′) and SsoFast EvaGreen Supermix (Bio-Rad, Hercules, CA) with a CFX96 real-time PCR detection system (Bio-Rad). To compare the relative amounts of viral RNA in a semi-quantitative manner, the cDNA was amplified using the same NS-specific primers described above, with AccuPower PCR premix (Bioneer, Daejeon, South Korea). The PCR products were separated on a 2% agarose gel. Images were acquired and the band intensities were measured using a Gel Doc XR^+ system with the Image Lab program (Bio-Rad).

2.5. Confocal microscopy

MDCK cells were infected with influenza virus PR8 at an MOI of 2.5 in the absence or presence of chemicals for 2.5 h at 37 °C. The cells were fixed with 4% paraformaldehyde and permeabilized with 0.1% Triton X-100. After blocking with 10% normal goat serum and 1% BSA in PBS, the slides were incubated overnight with an influenza A NP-specific monoclonal antibody (Santa Cruz Biotechnology, Santa Cruz, CA) at 4 °C and subsequently labeled with Alexa Fluor 488-conjugated goat anti-mouse IgG (Invitrogen) for 1 h at room temperature (RT). Before counterstaining with Vectashield mounting medium containing DAPI (Vector Laboratories, Burlingame, CA), actin was stained with Texas Red-conjugated phalloidin (Invitrogen). Laser scanning confocal microscopy was performed with a Zeiss LSM 710 confocal microscope and z-stack images were captured at intervals of 1 μm using the ZEN program (Carl Zeiss, Thornwood, NY). To determine the intracellular localization of the input virion-derived NP protein, 300 μg/ml of the protein synthesis inhibitor cycloheximide (Sigma) was added during the 5-h infection period at 37 °C.

2.6. Influenza viral polymerase activity assay

Based on previous reports, DNA derived from four PR8 genomic RNAs, including PB2, PB1, PA, and NP, were cloned individually into a vector that harbored convergent RNA polymerase I and II

promoters by RT-PCR using a universal reverse primer and genome-specific primers, which generated pVP-PB2, -PB1, -PA, and -NP, respectively (Hoffmann et al., 2000, 2001). The plasmid pHH21-EGFP, which expresses influenza virus-like RNA of EGFP (the negative strand of the EGFP mRNA is flanked by the 5′ and 3′ UTRs of NS) under the control of the human RNA polymerase I promoter, was constructed as described previously (Fujii et al., 2005; Pleschka et al., 1996). In brief, the EGFP gene was amplified from pEGFPLuc (BD Biosciences, Palo Alto, CA) using the following PCR primers: 5′-ATATCGTCTCGTATTAGTAGAAACAAGGGTGTTTTT-TATTATTACTTGTACAGCTCGTCCATGC-3′ and 5′-TATTCGTCTCAGG-GAGCAAAAGCAGGGTGACAAAGACATAATGGTGAGCAAGGGCGAG-GA-3′, and cloned into the *Bsm* BI sites of pHH21 (kindly provided by Dr. Gerd Hobom, Justus Liebig University, Giessen, Germany). The plasmid pHH21-FLuc, which expresses the virus-like RNA of the firefly luciferase (FLuc) gene, was prepared in the same manner, except FLuc-specific PCR primers were used (5′-ATATCGTCTCGTATTAGTAGAAACAAGGGTGTTTTTTATTATTACACGG CGATCTTTCCG CCCT-3′ and 5′-TATTCGTCTCAGGGAGCAAAAGCAGG GTGACAAAGACATAATGGAAGACGCCAAAAACAT-3′). To determine the effect of EGCG on the influenza virus polymerase activity, HEK 293T cells (4×10^5 cells per well in 12-well plates) were transfected with the four viral polymerases/NP-encoding pVP DNAs and pHH21-EGFP (0.4 μg each) using Lipofectamine 2000 (Invitrogen), according to the manufacturer's instructions. After 6 h, the supernatant was replaced with fresh medium containing dimethyl sulfoxide (DMSO) or compounds (EGCG and RBV at final concentrations of 100 μM). The fluorescent signals were measured at day 1 post-transfection using a Ti-E fluorescent microscope (Nikon Instruments). At the same time, Vero cells (5×10^5 cells per well in 12-well plates) were transfected with the four virus-derived DNAs and pHH21-FLuc (0.4 μg each), together with 0.1 μg of phLR-CMV (Promega, Madison, WI), which expressed *Renilla* luciferase (RLuc), according to the same protocol. After 6 h, fresh medium was added, which contained DMSO or increasing amounts of chemicals, *i.e.*, EGCG and favipiravir (T-705). On day

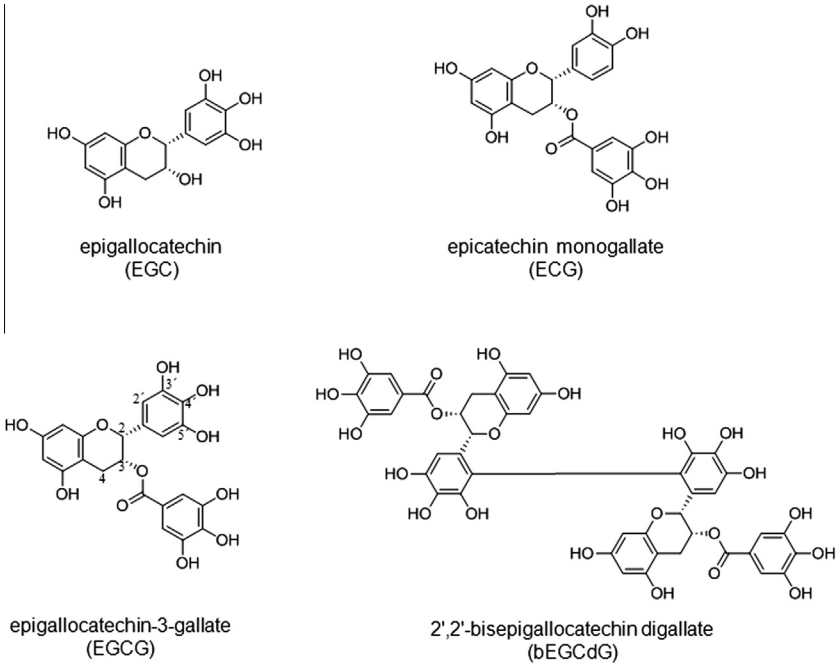

Fig. 1. Chemical structures of the catechin derivatives EGC, ECG, EGCG, and bEGCdG.

Table 1
Antiviral activity of catechin derivatives against influenza A/H1N1, A/H3N2 and B viruses infecting MDCK cells.[a]

Compound	EC_{50}[b] (μM) (S.I.[c])						CC_{50}[d] (μM)
	TW	PR8	BB	KR	HK	PNM	no virus
EGC	47.6 ± 13.2	>60	>60	n.t.[e]	>60	>60	>60
ECG	9.3 ± 0.5	41.0 ± 7.1	51.4 ± 0.6	n.t.	26.4 ± 1.1	45.4 ± 2.2	>60
EGCG	8.9 ± 0.6 (22.0)	10.0 ± 0.5 (19.6)	17.3 ± 3.2 (11.3)	5.8 ± 0.5 (33.8)	10.0 ± 2.3 (19.6)	5.7 ± 1.4 (34.4)	195.8 ± 6.7
bEGCdG	11.1 ± 0.8	10.3 ± 0.6	36.0 ± 0.4	n.t.	8.8 ± 0.8	34.8 ± 2.0	>60
AMT	0.51 ± 0.14	>100	0.55 ± 0.10	63.8 ± 12.7	0.74 ± 0.14	>100	>300
OSV-C	0.52 ± 0.06	0.22 ± 0.02	0.03 ± 0.00	<0.01	0.01 ± 0.00	0.08 ± 0.00	>300
RBV	42.3 ± 12.3	25.6 ± 6.8	20.4 ± 1.2	9.7 ± 3.4	22.8 ± 0.8	22.1 ± 11.2	>300
ARB	22.2 ± 2.0	n.t.	n.t.	n.t.	20.5 ± 1.4	>72.1	72.1 ± 12.2

[a] The data presented are the means ± standard deviations (SD) for two to five independent experiments.
[b] The EC_{50} is the 50% effective concentration, which is defined as the compound concentration that reduces the replication of influenza viruses by 50% in the CPE reduction assay.
[c] Selectivity index, CC_{50}/EC_{50}.
[d] The CC_{50} is the 50% cytotoxic concentration, which is defined as the compound concentration that produces cellular toxicity of 50%.
[e] n.t., not tested.

2 post-transfection, the FLuc activity was measured by normalizing against the RLuc activity using the dual-luciferase reporter assay system (Promega).

2.7. HA assay

Twenty-five microliters of two-fold diluted PR8 virus (HA titer, 256) were incubated with the same volume of PBS (a mock control), serially diluted EGCG, or an H1N1 HA1-specific monoclonal antibody (Abcam) at RT for 20 min. Next, each sample was mixed with 50 μl of 0.5% chicken RBCs. After 30 min incubation at RT, the concentration of EGCG or anti-HA1 antibody that inhibited the HA activity was measured. Three independent replicates of these experiments were performed.

2.8. Western blot analysis and bacterial NA treatment

To measure the relative amounts of cell-bound influenza virus, 500 μl of PR8 virus (2.5×10^5 PFU) was mixed with specific amounts of EGCG, or p-KG03 as a control, and added to MDCK cells (MOI = 0.2). After 1 h adsorption at 4 °C, the cells were washed twice with PBS and the lysates were harvested, before 12% sodium dodecyl sulfate polyacrylamide gel electrophoresis (SDS–PAGE) and electro-transfer to a polyvinylidene difluoride (PVDF) membrane. Viral HA2 protein and cellular β-actin (loading control) were detected using anti-HA2 (Sino Biological, Beijing, China) and anti-β-actin antibodies (Sigma), respectively.

The NA sensitivity assay was performed as described previously, with some modifications (Matlin et al., 1981; Wolkerstorfer

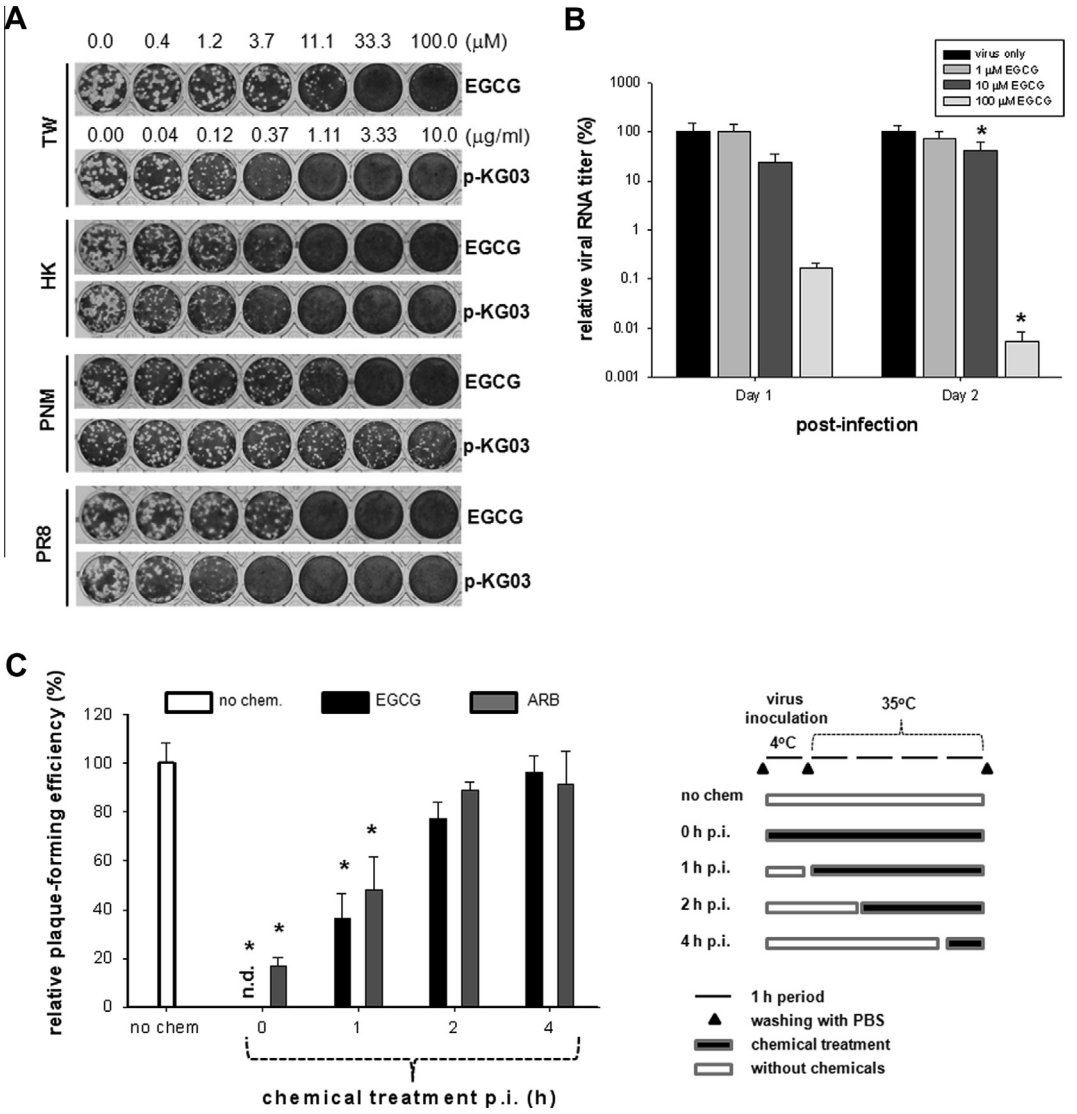

Fig. 2. Inhibition of influenza virus replication by EGCG. (A) A plaque inhibition assay was used to determine the antiviral activity of EGCG. MDCK cells were infected with different influenza viruses for 1 h at 33 °C (TW and PNM) or 35 °C (HK and PR8) in serum-free MEM. After washing with PBS, the cells were covered with overlay medium containing specified concentrations of EGCG or p-KG03 and incubated for an additional 2 or 3 days. Plaques were visualized by crystal violet staining. (B) Quantification of viral RNA titers in the culture medium. MDCK cells in 12-well plates were infected with influenza virus PR8 (MOI = 0.0006) at 35 °C for 1 h. The PR8-infected cells were washed with PBS and incubated in MEM in the absence (virus only) or presence of EGCG (1, 10, and 100 μM). The culture supernatants were harvested at days 1 and 2 p.i. The viral RNA titer was calculated by quantitative RT-PCR using viral NS-specific primers. The values shown are the means ± standard deviations (SD) for three different samples, which are expressed as percentages relative to the RNA titer without EGCG on each day. $^*p < 0.05$. (C) Time of addition experiments using EGCG. The experimental process is described in the panel on the right. MDCK cells were inoculated with influenza PR8 virus for 1 h at 4 °C in the presence or absence of EGCG to allow viral adsorption to the cell surface. After removal of the unadsorbed virus, the cells were incubated at 35 °C for an additional 4 h. At 1, 2, and 4 h p.i., 60 μM of EGCG or ARB was added to the cell culture medium. At 5 h p.i., the cell monolayers were washed with PBS and the overlay medium was added, before the plaque assay. The values shown are the means ± SD of duplicate samples, which are expressed as percentages relative to the plaque number without treatment. The data shown are representative of three independent experiments. n.d., not detectable. $^*p < 0.05$.

et al., 2009). In brief, the cells in six-well plates were infected with PR8 virus at an MOI of 0.2 in the absence or presence of antiviral agents (EGCG and ARB), either for 2 h at 4 °C (attachment) or 37 °C (attachment and internalization), or for 4 h at 37 °C (attachment, internalization, viral RNA replication, and early gene expression). After washing with ice-cold PBS, the cells were treated with 2.5 units per ml of *Clostridium perfringens* (*C. Perfringens*) NA (type V; Sigma) at 4 °C for 90 min. The cells were washed again with ice-cold PBS and the cell lysates were harvested, before being subjected to western blot analysis, as described above.

2.9. NA inhibition assay

PR8 virus (25 μl of 1×10^5 PFU/ml) or different types of purified NA proteins derived from *C. perfringens*, influenza H1N1 (A/California/04/2009) (Sino Biological), and its oseltamivir-resistant H275Y mutant (Sino Biological) in PBS [25 μl of 40 milliunits (mU) per ml] were mixed individually with an equal volume of serially diluted EGCG or OSV-C in 96-well plates. After adding 50 μl of 200 μM NA-Fluor fluorescent substrate (Applied Biosystems, Foster City, CA), the reaction mixture was incubated immediately at 37 °C for 1 h and stopped by the addition of 100 μl of stop solution. The fluorescence intensity was measured based on the excitation at 350 nm and the emission at 450 nm, according to the manufacturer's instructions. The half-maximum inhibitory concentration (IC_{50}) values were calculated using GraphPad Prism (GraphPad Software, La Jolla, CA).

2.10. Transmission electron microscopy and density analysis of the purified influenza virus

Influenza virus PR8 was purified by sucrose gradient ultracentrifugation, as described previously (Isaacs et al., 2008). In brief, 40 ml of embryonated chicken egg allantoic fluid inoculated with

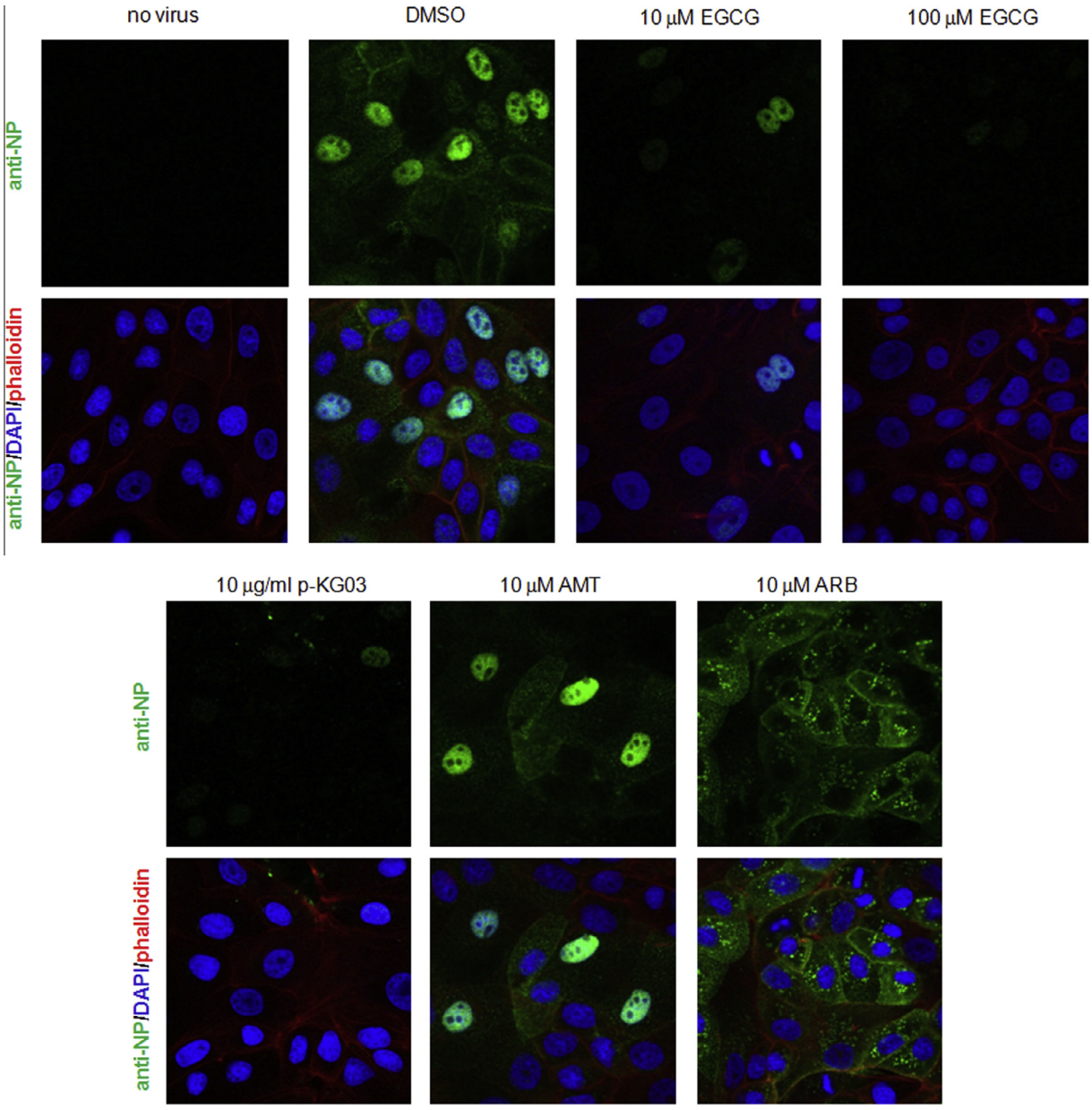

Fig. 3. EGCG-mediated inhibition of influenza virus entry. MDCK cells were mock-infected (no virus) or infected with PR8 virus (MOI = 2.5) in the presence of DMSO, EGCG, p-KG03, AMT, or ARB for 2.5 h at 37 °C. The viral NP protein was detected by confocal microscopy using a NP-specific monoclonal antibody and Alexa 488-conjugated goat anti-mouse secondary antibody (green). Actin was stained with Texas red-labeled phalloidin (Red). Nuclei were counterstained with DAPI (blue). Original magnification, 400×.

influenza virus (5×10^6 PFU/ml) was clarified by centrifugation at 2500 rpm for 10 min. The virus was precipitated by centrifugation at 19,000×*g* for 2 h in a JA-20 rotor (Beckmann Instruments, San Ramon, CA). The virus pellet was suspended in 1 ml TNE buffer [50 mM Tris–HCl (pH 7.4), 100 mM NaCl, and 1 mM EDTA], and loaded onto a sucrose gradient (2 ml of 50%, 40%, and 30% sucrose dissolved in TNE buffer). After centrifugation at 36,000×*g* for 2 h in an SW-41 rotor (Beckmann), the fractions were collected (750 μl per fraction) and the virus-containing fractions were pooled after confirmation by western blot analysis. The samples collected were diluted five-fold with PBS and centrifuged again in a Beckmann SW-41 rotor at 82,000×*g* for 1 h. The virus pellet was finally resuspended in 4 ml of PBS.

Before the transmission electron microscopy (TEM) analysis, 100 μl of the purified PR8 virus (approximately 2×10^7 PFU/ml) was mixed with 1 μl of DMSO, or with 1 μl of 10 mM or 50 mM of EGCG (final concentrations of 100 μM and 500 μM, respectively), at RT for 1 h. Each sample (5 μl) was applied to a glow discharge, carbon-coated electron microscopy grid. The samples were adsorbed for 1 min onto the carbon support film. The grid was washed with three droplets of water and 5 μl of 1% (w/v) uranyl acetate solution was applied to the grid. After staining for 1 min, the excess stain solution was blotted away using a piece of filter paper. Specimens were examined using a Tecnai G^2 Spirit Twin electron microscope (FEI Company, Hillsboro, OR), which was equipped with an LaB6 filament and operated at an accelerating voltage of 120 kV. Images were recorded using an UltraScan 4000 charge coupled device (CCD) detector (Gatan, Pleasanton, CA) at magnifications of 6500× (1.59 nm/pixel) and 30,000× (0.36 nm/pixel). The viral particle size was determined by calculating the average diameter of 100 different particles from each sample.

To measure the change in the influenza virus density, purified PR8 virus (2×10^7 PFU/ml) was mixed with DMSO or EGCG (final concentration of 500 μM) at 37 °C for 2 h. After ten-fold dilution with TNE buffer, the samples were loaded onto a discontinuous 30%, 40%, and 50% sucrose gradient and centrifuged at 82,000×*g* for 1 h in an SW-41 rotor (Beckmann). The fractions were analyzed by western blotting using anti-HA2, -HA1, and -NP antibodies (anti-HA2 and -NP purchased from Sino Biological; anti-HA1 purchased from Abcam, Cambridge, MA), and by semi-quantitative RT-PCR using NS-specific primers described earlier.

2.11. Statistical analysis

Statistically significant differences were determined using a one-tailed Student's *t*-test. $P < 0.05$ was considered significant.

3. Results

3.1. Anti-influenza virus activity of catechin derivatives

The antiviral activities of EGCG and other catechin derivatives, such as EGC, ECG, and bEGCdG, were tested against human influenza A (A/H1N1: TW, PR8, BB, and KR; A/H3N2: HK) and B (PNM) viruses using a CPE reduction assay (Fig. 1 and Table 1). The results showed that EGCG had the most significant effects in reducing both type A and B influenza virus replication in MDCK cells, with EC_{50} values ranging from 5.7 to 17.3 μM. Both bEGCdG and ECG were also active, but their inhibitory effects varied depending on the viral isolates. By contrast, EGC was inactive even at the highest concentration tested (60 μM), except against the TW virus, where it had a marginal EC_{50} of 47.6 μM. The antiviral activity profile of the monomeric compounds decreased in the following order: EGCG > ECG > EGC, which are similar to the effects observed against HSV-2 and influenza virus isolates in previous studies (Isaacs et al., 2008; Song et al., 2005). Although dimeric EGCG, bEGCdG, was less potent against the BB and PNM strains, its inhibitory effects against TW, PR8, and HK were comparable to that of monomeric EGCG. Thus the 2′ position of the trihydroxyphenyl moiety, which is linked at position 2 of EGCG, appears to be accessible for chemical modification if increased antiviral potency is required. In addition, the MDCK cell viability was reduced by 50% with an EGCG concentration of 195.8 μM, which suggests that the selectivity index for influenza virus ranged from 11.3 to 34.4 (Table 1).

To study the antiviral activity of EGCG, its purity (⩾95%) and molecular weight (458.4 Da) were confirmed by LC–MS (data not

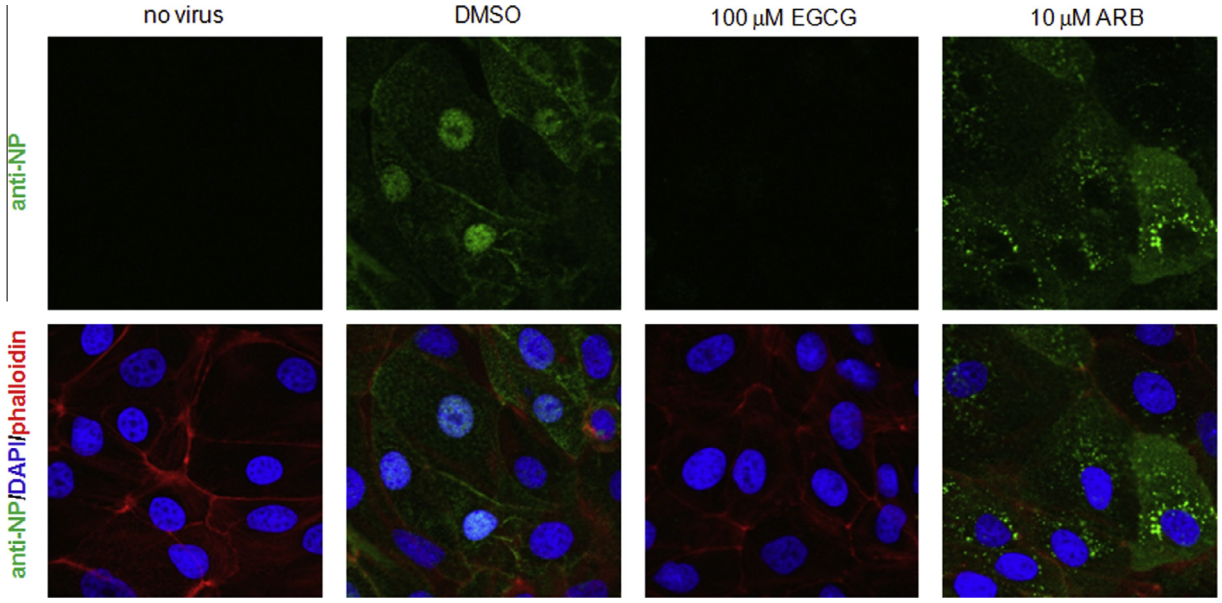

Fig. 4. Monitoring the reduction of influenza virus entry due to EGCG in a protein synthesis-arrested condition. Cells were infected with PR8 virus at an MOI of 2.5 in the presence of DMSO, 100 μM EGCG, or 10 μM ARB in MEM containing 300 μg/ml cycloheximide for 5 h at 37 °C. The viral NP protein, cell nuclei, and membranes are labeled in green, blue, and red, respectively. Original magnification, 400×.

shown). Next, tests were conducted to determine whether EGCG inhibits influenza virus infection directly, using a plaque inhibition assay and quantitative real-time RT-PCR (Fig. 2A and B). A sulfated polysaccharide, p-KG03, which is a known inhibitor of influenza virus entry (except PNM), was used as a positive control (Kim et al., 2012). As shown in a previous study (Song et al., 2005), the efficiency of plaque formation by the TW, HK, PNM, and PR8 strains declined in an EGCG concentration-dependent manner, with EC_{50} values of 14.9 ± 1.1, 4.3 ± 0.1, 13.2 ± 1.1, and 5.5 ± 0.2 μM, respectively. These values were distributed in very similar ranges to those obtained in the CPE assay (Table 1). It was also found that the viral RNA titers in the culture supernatants were reduced in the presence of EGCG (Fig. 2B).

The step in the viral replication cycle affected by EGCG was identified based on its addition to virus-infected cells at different time points, *i.e.*, 0, 1, 2, and 4 h p.i., using ARB as a control compound, which is a HA2-associated fusion inhibitor (Leneva et al., 2009) (Fig. 2C). The two compounds had similar time-dependent antiviral effect profiles. Their antiviral activity was significant when added within 1 h p.i., whereas they had little or no effects on influenza virus infection at later time points. These results suggest that EGCG targets the early steps of virus infection, which do not occur after virus-endosome fusion.

3.2. Inhibition of influenza virus entry by EGCG

The effect of EGCG on influenza virus entry was evaluated by confocal microscopy using NP-specific antibodies. As shown in Fig. 3, the NP protein was localized efficiently to the nucleus with only a minor distribution in the cytoplasm at 2.5 h p.i. ('no virus' vs. 'DMSO'). However, the NP protein signal declined noticeably in the presence of 10 μM EGCG and more dramatically in the presence of 100 μM EGCG, which was similar to the effect observed with the entry inhibitor p-KG03. As expected, the NP protein of

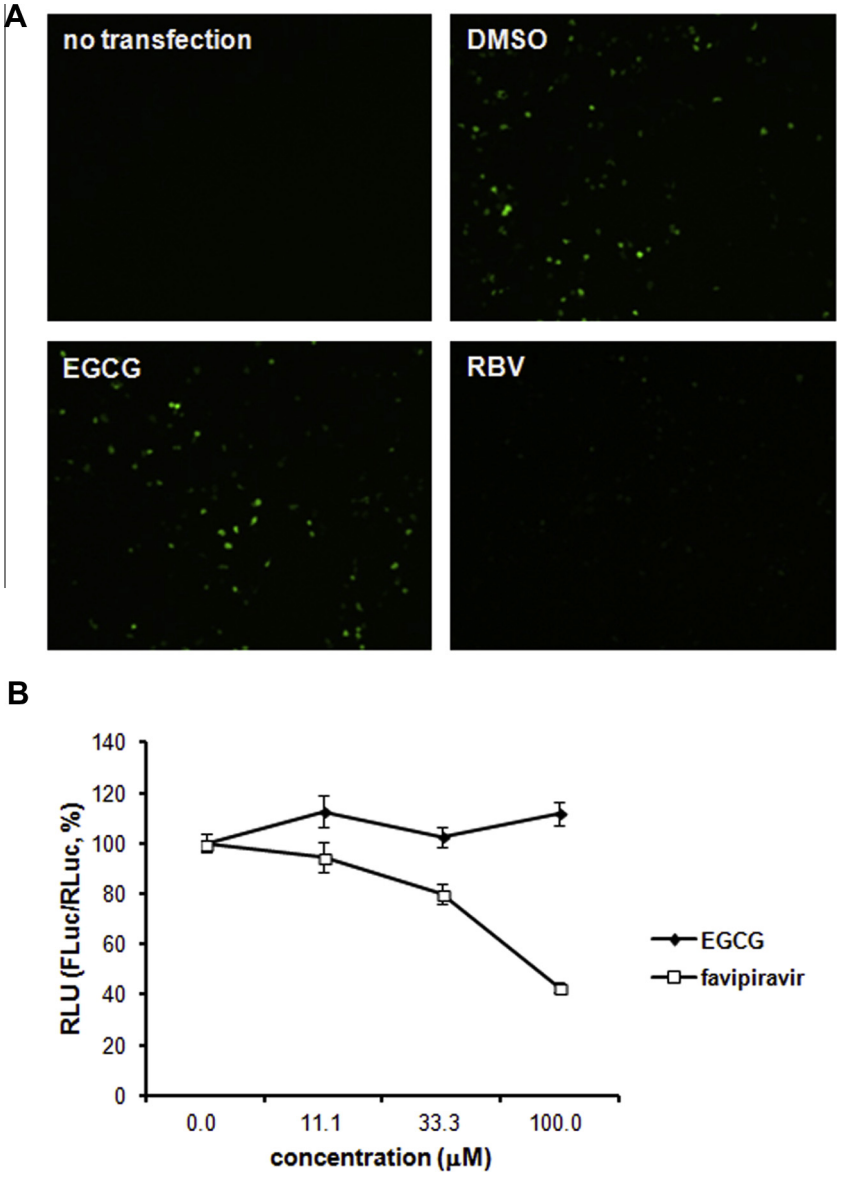

Fig. 5. No effect of EGCG on viral polymerase activity. (A) HEK 293T cells seeded in 12-well plates were transfected with the mock treatment (no transfection) or pVP-PB2, -PB1, -PA, -NP, and pHH21-EGFP (0.4 μg each). At 6 h, DMSO, or 100 μM of EGCG or RBV, was added to each well. At day 1 after transfection, EGFP expression was assessed by fluorescence microscopy. Original magnification, 100×. (B) Vero cells in 12-well plates were transfected with the same plasmid DNAs, except 0.4 μg of pHH-FLuc and 0.1 μg of phRL-CMV (as a transfection control) were substituted for the pHH-EGFP used above. At 6 h, DMSO or increasing amounts of EGCG or favipiravir (11, 33, and 100 μM) were added to each well. The FLuc expression level in cells was normalized against that of RLuc on day 2.

the AMT-resistant PR8 virus localized to the nucleus, irrespective of the AMT treatment. By contrast, ARB did not affect viral infection but it induced the cytoplasmic arrest of NP. These findings indicate that the mechanism that allows ARB to inhibit virus entry is different from that used by EGCG. This is because EGCG did not affect the intracellular distribution pattern of NP, but it did reduce its intensity within the nucleus in a dose-dependent manner.

However, it was possible that the NP signal was attributable to newly synthesized NP and that its reduction was caused by the inhibition of viral RNA replication and protein translation by EGCG. Thus, confocal microscopy was repeated in the presence of cycloheximide, a protein synthesis inhibitor. The microscopic analysis showed clearly that, in the absence of protein synthesis, entry of the viral NP protein was blocked by treatment with EGCG, whereas treatment with ARB resulted in the accumulation of NP protein in the cytoplasm (Fig. 4). In addition, the effect of EGCG on viral polymerase was studied using two different types of reporter system expressing virus-like RNAs of EGFP or FLuc, with a cell culture-based viral polymerase assay (Fujii et al., 2005; Hoffmann et al., 2000). The data suggested that the activity of influenza polymerase was not affected by EGCG (Fig. 5). Overall, these results indicate that EGCG inhibits influenza virus entry but not virus-endosome fusion or viral RNA replication.

3.3. No effect of EGCG on influenza virus binding to the cell surface

Adsorption of influenza virus to cells was studied to identify the viral entry step controlled by EGCG. MDCK cells were incubated at 4 °C for 1 h with increasing amounts of EGCG or the adsorption inhibitor p-KG03. The cell lysates were subjected to western blot analysis to detect the cell surface-bound viral HA2 protein (Fig. 6A). Interestingly, as expected p-KG03 inhibited viral binding to the cells in a dose-dependent manner, whereas EGCG had no effect on PR8 influenza virus adsorption. Similarly, the ability of PR8 HA to agglutinate chicken RBCs was not affected by EGCG compared with an HA1-specific neutralizing antibody, which reduced the HA titers from 256 to 128 per 25 μl at a concentration of 0.6 μg/ml, 64 at 1.3 μg/ml, 16 at 2.5 μg/ml, and 8 at 5.0 μg/ml (Fig. 6B). This finding was also confirmed using other influenza strains TW, HK, PNM, and BB (data not shown). The HA assay also showed that EGCG is toxic to erythrocytes at concentrations above 50 μM, so its inhibitory effect on the activity of viral HA is not permissible at higher concentrations.

3.4. Membrane penetration of influenza virus is prevented by EGCG

To determine whether EGCG prevents viral particles attached to the cell surface from being internalized, the distributions of viral particles were analyzed after treatment with *C. perfringens* (Cp) NA, which is known to hydrolyze α(2 → 3), α(2 → 6), and α(2 → 8)-glycosidic linkages, and to selectively remove receptor-bound influenza virions (Matlin et al., 1981; Wolkerstorfer et al., 2009). MDCK cells were inoculated with the virus at 4 °C and 37 °C in the absence or presence of EGCG and ARB, and then treated with Cp NA. In agreement with earlier results (Fig. 6A), incubation at 4 °C with either EGCG or ARB did not affect virus binding to cells (Fig. 7A, left). Interestingly, no viral HA2 protein was removed from the cell surface of EGCG-treated cells after treatment with the NA (Fig. 7A, lanes 8 and 9), whereas it was washed away completely in mock- or ARB-treated samples (Fig. 7A, lanes 7, 10, and 11), thereby demonstrating the enzymatic efficacy of the added Cp NA protein. After infection at 37 °C for 2 h without NA treatment, the viral HA2 protein levels varied among samples, with a distinctive accumulation trend in the EGCG samples (Fig. 7B, left). This trend was also apparent after treatment with Cp NA (Fig. 7B, right). Given the confocal microscopy data (Figs. 3 and 4), the HA2 band present in the mock sample (Fig. 7B, lane 7) may have been derived mainly from normally internalized virions, whereas those present in EGCG-treated samples (Fig. 7B, lanes 8 and 9) may have been derived from non-internalized virions, and those with the ARB

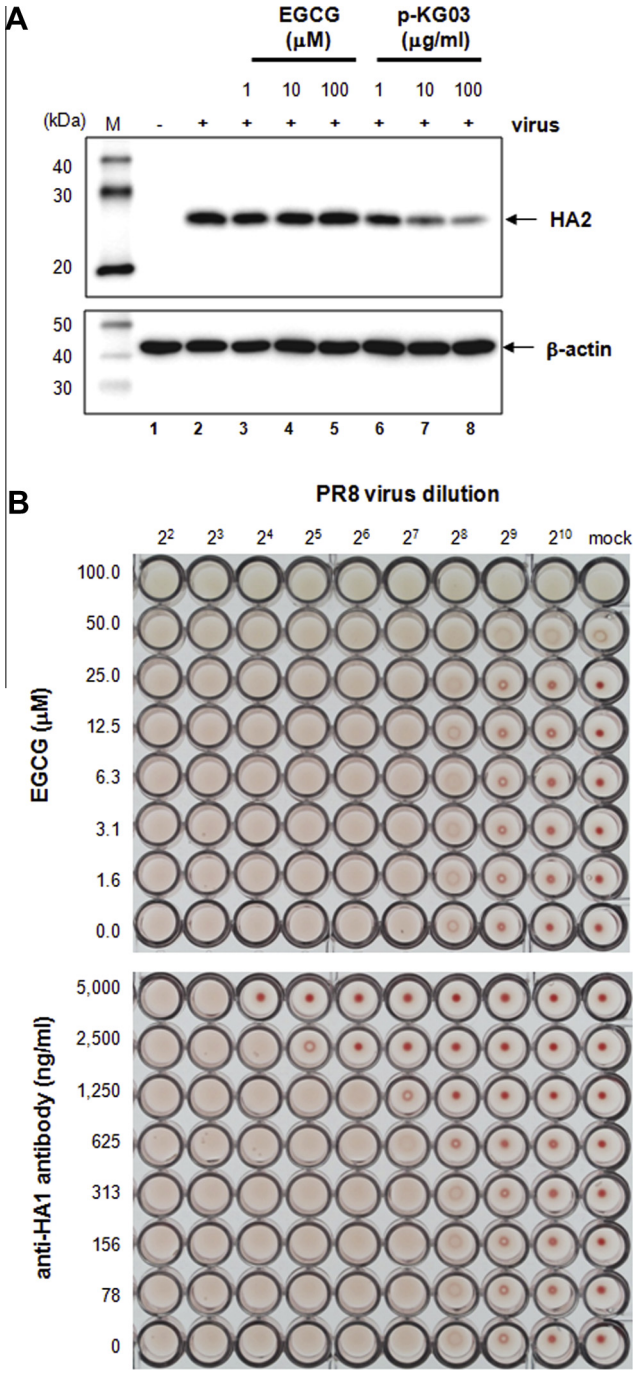

Fig. 6. Effects of EGCG on influenza virus binding to cells. (A) Western blot analysis. MDCK cells were mock-infected (−virus) or infected with PR8 (+virus) in the presence of increasing amounts of EGCG or p-KG03 for 1 h at 4 °C. After washing with ice-cold PBS, the total cell lysates were harvested and subjected to 12% SDS–PAGE. Viral HA2 and cellular β-actin (loading control) proteins were detected using specific antibodies and HRP-conjugated secondary antibodies. The molecular weights of the markers (M) are indicated on the left of the panels. (B) HA activity assay. Two-fold diluted PR8 virus was incubated with an equal volume of serially diluted EGCG or anti-HA antibody in PBS for 20 min. Red blood cells (RBCs) were then added to each well at a final concentration of 0.25%. The viral HA-mediated RBC agglutination was monitored after further incubation for 30 min at room temperature.

treatment (Fig. 7B, lanes 10 and 11) could have originated from virions that did not undergo membrane fusion in the cytoplasm. This was confirmed by harvesting cell lysates after an extended incubation period (4 h) at 37 °C (Fig. 7C), which was sufficient to allow the early expression of viral proteins, such as HA0, from internalized viral genome segment 4 (Fig. 7C, lane 2). The expression of the newly synthesized full-length HA0 protein was reduced in a dose-dependent manner by either EGCG or ARB treatment (Fig. 7C, lanes 3–6). As shown in the right panel of Fig. 7C, both the HA0 and HA2 proteins were insensitive to NA treatment. This indicates that they are localized within the cell, with the exception of HA2 in EGCG-treated samples, which might be tethered to the cell membrane in a NA-resistant state. Overall, these data suggest that both EGCG and ARB inhibit the entry of viral particles, but that they use different mechanisms: EGCG fixes the influenza virus to the cell surface, whereas ARB interrupts the migration of the viral ribonucleoprotein complex from the cytoplasm to the nucleus *via* blocking HA2-mediated membrane fusion.

To determine why EGCG causes defects in influenza virus NA-mediated internalization, an NA activity assay was performed using whole PR8 virus and purified viral [A/California/04/2009 (H1N1)], or nonviral Cp NA proteins, with increasing amounts of EGCG or OSV-C (Fig. 8). Interestingly, EGCG antagonized the activity of influenza virus NA, as reported previously (Song et al., 2005), but also that of bacterial NA (Fig. 8A). The wild-type and OSV-resistant mutant (H275Y) NA proteins were inhibited by EGCG. However, compared with the confocal microscopy analyses (Figs. 3 and 4) or western blot experiments (Figs. 6 and 7), which used similar virus titers to those employed in this assay, much higher concentrations of EGCG were required to induce sufficient NA inhibition: EGCG had IC_{50} values of >500 μM against PR8, 133.2 ± 1.0 μM against Cp, 145.3 ± 1.1 μM against NA, and 233.7 ± 1.0 μM against NA(275Y). These results suggest that although the NA inhibitory effect of EGCG could contribute partially to the suppression of virus entry, it is not considered to be a major factor because of its high IC_{50} values.

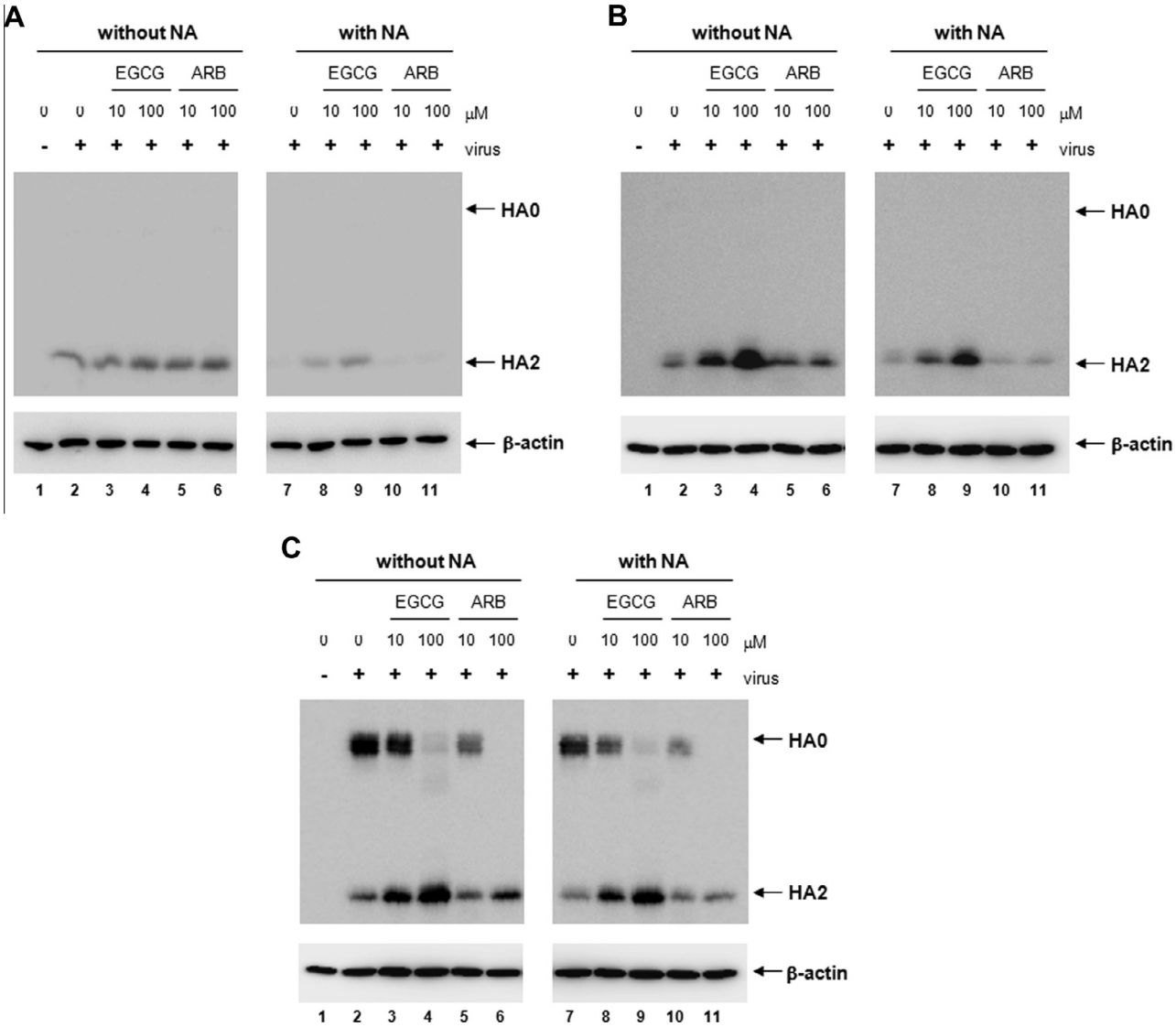

Fig. 7. Inhibition of influenza virus internalization by EGCG. Confluent MDCK cells were seeded in six-well plates and mock-infected (−virus) or infected with influenza virus (+virus) at an MOI of 0.2 in the absence or presence of chemicals (EGCG and ARB) for 2 h at 4 °C (A) or 37 °C (B), or for 4 h at 37 °C (C). After washing with PBS, the cells were either harvested immediately (without NA) or after incubation with 1 ml of MEM containing *Clostridium perfringens* NA (2.5 units/ml) for 90 min at 4 °C (with NA). The total cell lysates were separated by 12% SDS–PAGE and the viral HA and cellular β-actin (loading control) proteins were detected by western blot analysis using their specific antibodies. The positions of HA0, HA2, and β-actin proteins in the gels are indicated on the right of the panels.

3.5. Morphological and physical analysis of influenza virus in the presence of EGCG

The PR8 virus was purified by sucrose density gradient centrifugation to investigate the physical effects of EGCG on the influenza virus. The highly concentrated influenza virus (2×10^7 PFU/ml) was incubated with DMSO or EGCG at RT for 1 h, followed by negative staining with uranyl acetate and TEM analysis (Fig. 9). The results showed that 2% DMSO, which was used as a solvent for EGCG and was present in all of the test samples, slightly reduced the viral particle size but had no effect on the viral morphology. The mock- and DMSO-treated controls were ball-like, rounded particles with average particle diameters of 152.6 ± 35.5 nm and 140.2 ± 23.2 nm, respectively (Fig. 9A, B, E, and F). There was no statistically significant difference between the two groups. However, when the virus was treated with EGCG, the negatively-stained particles assumed a doughnut-like shape, which indicated the enhanced permeation of the staining solution into the viral core, possibly due to viral lipid membrane damage (Fig. 9C, D, G, and H). In samples treated with 100 μM and 500 μM EGCG, the particle diameters decreased to 138.3 ± 26.4 nm (not significantly different compared with the DMSO treatment) and 125.0 ± 19.8 nm ($p < 0.00001$, significantly different compared with the DMSO treatment), respectively. Given that the viral titers used for TEM analysis (2×10^7 PFU/ml) were 800-fold higher than those used in the NA assay (2.5×10^4 PFU/ml), with 40% inhibition at 500 μM EGCG (Fig. 8), these physical changes in the overall viral particle population at the same concentration are noteworthy (Fig. 9D and H).

To determine whether the decrease in the particle size was involved with the change in the particle density, purified high virus titers were incubated with 2% DMSO or 500 μM EGCG at 37 °C for 2 h and subjected to additional sucrose gradient ultracentrifugation. The changes in the density of the viral particles in these two samples were monitored by measuring the relative amounts of viral HA2, HA1, and NP proteins, as well as the levels of viral RNA in each fraction, by western blot and semi-quantitative RT-PCR analyses. As shown in Fig. 10, fraction 6 contained the highest abundance of all three viral proteins and the viral genome. After treatment with EGCG, however, these components moved to the denser fraction 7. Thus, the TEM and viral density analyses suggest that the antiviral activity of EGCG might be attributable to its ability to impair the viral membrane and the physical properties of the influenza particles.

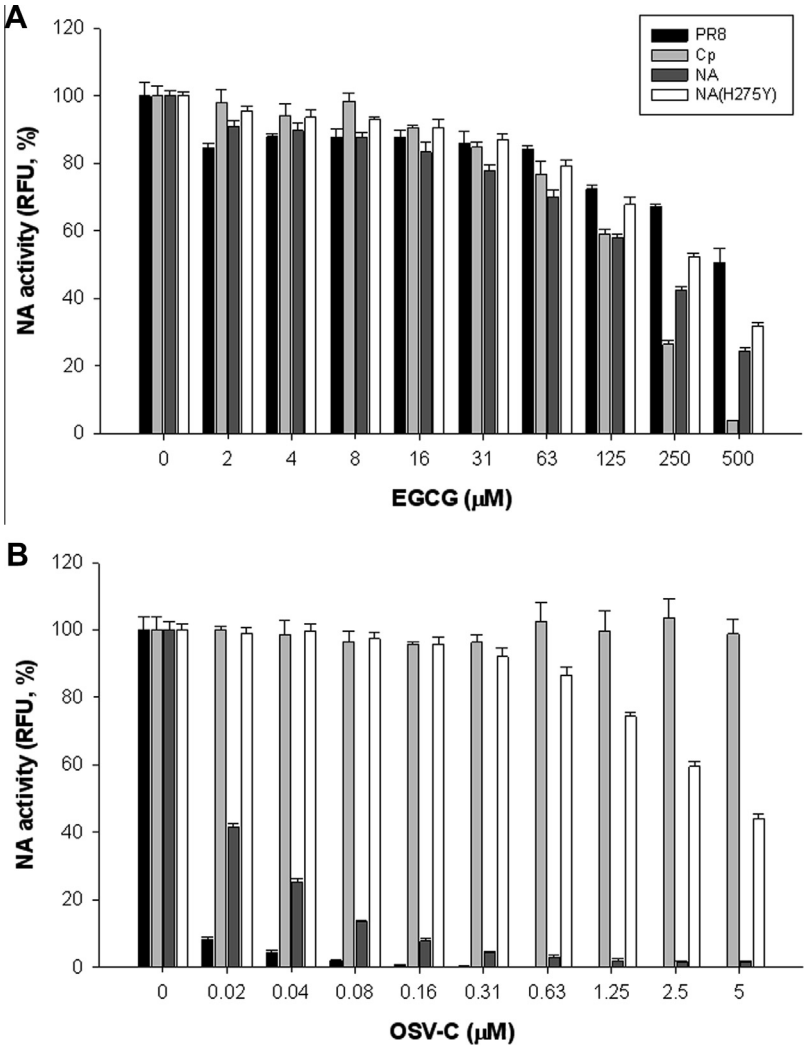

Fig. 8. NA activity assay. The enzymatic activity of the PR8 virus, *C. perfringens* NA (Cp), or purified influenza viral NA protein, *i.e.*, wild-type (NA) or mutant [NA(H275Y)], were measured in the presence of increasing amounts of EGCG (A) or OSV-C (B). After adding the NA-Fluor fluorescent substrate, the activity was determined by measuring the fluorescence intensity with excitation at 350 nm and emission at 450 nm. The data shown are the means ± SD for three different samples.

4. Discussion

The antiviral effects of EGCG have been reported to be mediated mainly by preventing the envelope glycoproteins of viruses, including those of HSV and HCV, from binding to their cell surface receptors. EGCG has also been shown to target the cell surface receptor CD4 and to interfere with HIV-1 gp120 recognition (Calland et al., 2012; Isaacs et al., 2008; Kawai et al., 2003; Song et al., 2005). In terms of its anti-influenza activity, EGCG has been proposed to suppress not only the ability of HA protein but also the effects of viral RNA polymerase complex and NA protein (Nakayama et al., 1993; Song et al., 2005). In the present study, it was shown that EGCG regulates influenza virus entry at a step before early membrane fusion (Figs. 2–4). The antiviral activity mode was not related to its effects on the function of viral polymerase or HA-mediated virus adsorption (Figs. 5 and 6). Thus, two possible mechanisms might explain the defective internalization of influenza virus particles caused by EGCG. First, EGCG inactivates the

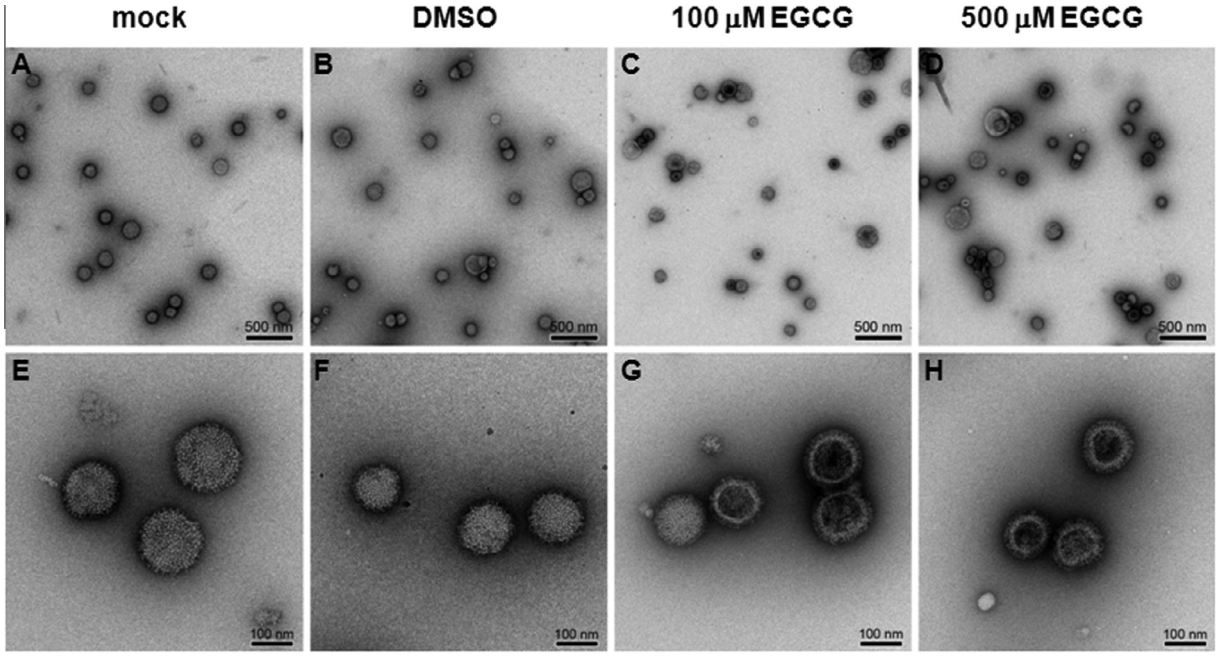

Fig. 9. TEM analysis. Purified PR8 virus alone (A and E) or with DMSO (B and F) or with different concentrations of EGCG (C, D, G, and H) was incubated in PBS at room temperature for 1 h. The samples were spread on a carbon-coated grid and stained with uranyl acetate before TEM analysis. The images were captured at magnifications of 6500× (scale bar = 500 nm; A–D) and 30,000× (scale bar = 100 nm; E–H).

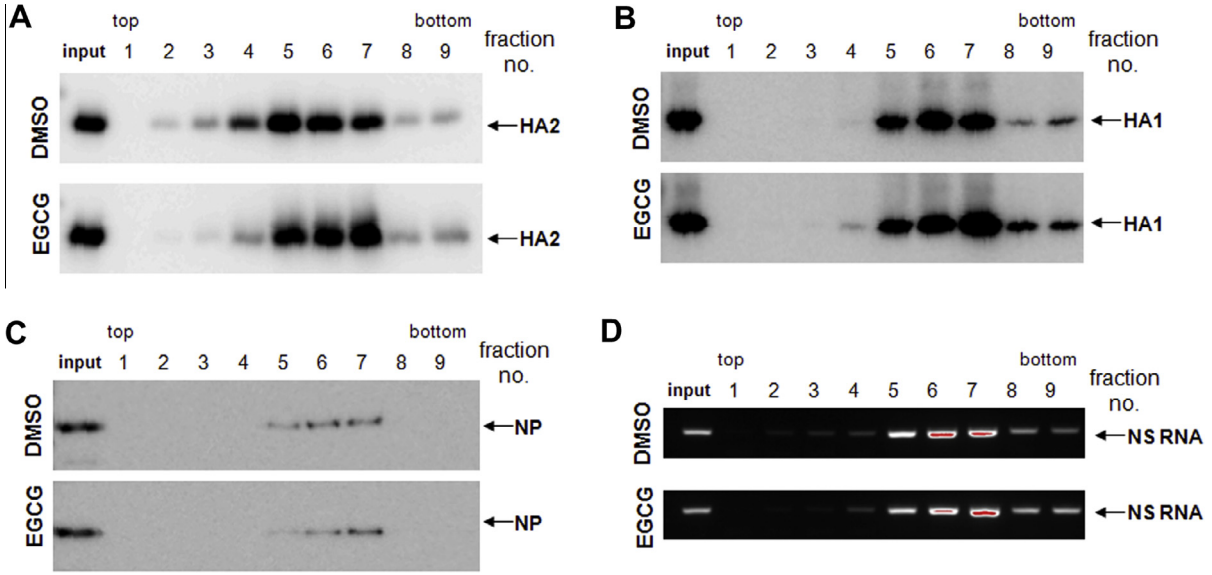

Fig. 10. Ultracentrifugation analysis of purified influenza virus. Purified influenza virus PR8 in 100 μl PBS (2×10^7 PFU/ml) was incubated with DMSO or EGCG at 37 °C for 2 h. The virus samples were diluted ten times with TNE buffer (final volume = 1 ml) and loaded onto a 50%, 40%, and 30% sucrose gradient in TNE (2 ml each), followed by density-based separation of the samples by ultracentrifugation at 82,000×*g* for 1 h at 4 °C. All fractions [top (fraction 1) to bottom (fraction 9)] were subjected to western blot analysis and semi-quantitative RT-PCR to detect the viral proteins, HA2 (A), HA1 (B), and NP (C), and the viral RNA genome NS (D). In (D), any amplified DNA bands that exceeded the detection sensitivity were highlighted automatically in red by the analysis software.

viral NA protein, which cleaves the cell surface sialic acid moiety linked to the virus and promotes internalization (Ohuchi et al., 2006). Second, EGCG induces physical damage to the virus particles, possibly the lipid bilayers, which may result in the loss of their hemifusion capacity and protrusion properties. The extended mode of action analyses conducted showed that EGCG controls the internalization of virus particles by impairing the rigidity and permeability of the viral membrane, with marginal inhibition of the NA activity (Figs. 7–9). In particular, the cell surface-bound influenza virus particles were resistant to NA in the presence of EGCG and even after EGCG was removed (Fig. 7), which indicates that the structure of the HA-sialic acid linkage might be damaged irreversibly. The direct effects of EGCG on viral particles were examined, which showed that EGCG altered the viral particle size and density by modifying the viral membrane integrity, rather than by disrupting the rounded morphology of particles (Figs. 9 and 10). In agreement with this observation, EGCG-mediated membrane damage was proposed in a previous report, which found that EGCG solubilized artificially formulated lipid bilayers without forming pores (Sun et al., 2009). Thus, previous findings of HA inhibition by EGCG (Nakayama et al., 1993; Song et al., 2005) might be explained by the long-term preincubation of virus with EGCG, which means that conformational changes in the active HA protein might have occurred due to the collapse of the lipid bilayer rather than the direct interaction between EGCG and viral HA.

In a recent study, NF-E2-related factor 2 (Nrf2), a cellular transcription factor of antioxidant heme oxygenase-1, was proposed to suppress influenza virus entry and replication in cells (Kesic et al., 2011). It was shown that the anti-influenza activity of Nrf2 was enhanced by EGCG, which is a natural antioxidant. In a preliminary study, however, we found that EGCG did not affect the cellular factors required for viral infection because there was little or no effect on the influenza virus infectivity in cells treated with EGCG before infection (data not shown). These contrasting results may be explained by differences in the EGCG treatment times or cell types. For example, the MDCK cells were pretreated for 1 h before viral infection in our experiments, whereas Kesic et al. pretreated primary human nasal epithelial cells for 3 h before virus infection to allow sufficient stimulation of Nrf2. In addition, it was suggested that EGCG could control the viral RNA replication efficacy by upregulating the expression of interferon-β and retinoic acid inducible gene I (Kesic et al., 2011). Other researchers have also proposed that EGCG can inhibit the viral polymerase activity, potentially by antagonizing the endonuclease protein component, PA (Kuzuhara et al., 2009; Song et al., 2005). However, the cell-based viral RNA polymerase assays conducted in the present study using a minireplicon system showed that EGCG did not influence the activity of the influenza virus polymerases/NP complex directly (Fig. 5). Thus, the inhibition of viral RNA replication and protein expression by EGCG might have been attributable to its effects on other viral proteins, such as nonstructural protein 1 (NS1), which was excluded from our polymerase assay system. However, it is possible that the efficacy of EGCG delivery into cells varies widely among different cell types, which could affect polymerase inhibition by EGCG.

In conclusion, the results study suggest that EGCG has potential as an anti-influenza drug because it damages the viral membrane and blocks viral penetration into cells. This pathway is distinct from the currently available antiviral therapeutics, such as NA or M2 inhibitors. EGCG was toxic to chicken RBCs at concentrations above 50 μM, but it was sufficiently active at sub-toxic concentrations, with EC_{50} values lower than 17.3 μM against various influenza virus isolates. Thus, if the therapeutic window can be optimized *in vivo*, EGCG or its chemically modified versions could be tested as a single or combination therapy for the treatment of currently circulating influenza virus strains, including drug-resistant viruses.

Acknowledgments

We would like to thank the staff at the Korea Chemical Bank of the Korea Research Institute of Chemical Technology for supplying the test compounds and for characterizing their purity and identity. This work was supported by the Transgovernmental Enterprise for Pandemic Influenza in Korea (TEPIK) (Grant A103001).

References

Cabrera, C., Artacho, R., Gimenez, R., 2006. Beneficial effects of green tea – a review. J. Am. Coll. Nutr. 25, 79–99.
Calland, N., Albecka, A., Belouzard, S., Wychowski, C., Duverlie, G., Descamps, V., Hober, D., Dubuisson, J., Rouille, Y., Seron, K., 2012. (−)-Epigallocatechin-3-gallate is a new inhibitor of hepatitis C virus entry. Hepatology 55, 720–729.
Chen, C., Qiu, H., Gong, J., Liu, Q., Xiao, H., Chen, X.W., Sun, B.L., Yang, R.G., 2012. (−)-Epigallocatechin-3-gallate inhibits the replication cycle of hepatitis C virus. Arch. Virol. 157, 1301–1312.
Cho, E.J., Xia, S., Ma, L.C., Robertus, J., Krug, R.M., Anslyn, E.V., Montelione, G.T., Ellington, A.D., 2012. Identification of influenza virus inhibitors targeting NS1A utilizing fluorescence polarization-based high-throughput assay. J. Biomol. Screen. 17, 448–459.
Ciesek, S., von Hahn, T., Colpitts, C.C., Schang, L.M., Friesland, M., Steinmann, J., Manns, M.P., Ott, M., Wedemeyer, H., Meuleman, P., Pietschmann, T., Steinmann, E., 2011. The green tea polyphenol, epigallocatechin-3-gallate, inhibits hepatitis C virus entry. Hepatology 54, 1947–1955.
De Clercq, E., 2006. Antiviral agents active against influenza A viruses. Nat. Rev. Drug Discov. 5, 1015–1025.
Fujii, K., Fujii, Y., Noda, T., Muramoto, Y., Watanabe, T., Takada, A., Goto, H., Horimoto, T., Kawaoka, Y., 2005. Importance of both the coding and the segment-specific noncoding regions of the influenza A virus NS segment for its efficient incorporation into virions. J. Virol. 79, 3766–3774.
Hauber, I., Hohenberg, H., Holstermann, B., Hunstein, W., Hauber, J., 2009. The main green tea polyphenol epigallocatechin-3-gallate counteracts semen-mediated enhancement of HIV infection. Proc. Natl. Acad. Sci. USA 106, 9033–9038.
Hoffmann, E., Neumann, G., Kawaoka, Y., Hobom, G., Webster, R.G., 2000. A DNA transfection system for generation of influenza A virus from eight plasmids. Proc. Natl. Acad. Sci. USA 97, 6108–6113.
Hoffmann, E., Stech, J., Guan, Y., Webster, R.G., Perez, D.R., 2001. Universal primer set for the full-length amplification of all influenza A viruses. Arch. Virol. 146, 2275–2289.
Hurt, A.C., Chotpitayasunondh, T., Cox, N.J., Daniels, R., Fry, A.M., Gubareva, L.V., Hayden, F.G., Hui, D.S., Hungnes, O., Lackenby, A., Lim, W., Meijer, A., Penn, C., Tashiro, M., Uyeki, T.M., Zambon, M., 2012. Antiviral resistance during the 2009 influenza A H1N1 pandemic: public health, laboratory, and clinical perspectives. Lancet Infect. Dis. 12, 240–248.
Isaacs, C.E., Wen, G.Y., Xu, W., Jia, J.H., Rohan, L., Corbo, C., Di Maggio, V., Jenkins Jr., E.C., Hillier, S., 2008. Epigallocatechin gallate inactivates clinical isolates of herpes simplex virus. Antimicrob. Agents Chemother. 52, 962–970.
Kawai, K., Tsuno, N.H., Kitayama, J., Okaji, Y., Yazawa, K., Asakage, M., Hori, N., Watanabe, T., Takahashi, K., Nagawa, H., 2003. Epigallocatechin gallate, the main component of tea polyphenol, binds to CD4 and interferes with gp120 binding. J. Allergy Clin. Immunol. 112, 951–957.
Kesic, M.J., Simmons, S.O., Bauer, R., Jaspers, I., 2011. Nrf2 expression modifies influenza A entry and replication in nasal epithelial cells. Free Radic. Biol. Med. 51, 444–453.
Kim, M., Yim, J.H., Kim, S.Y., Kim, H.S., Lee, W.G., Kim, S.J., Kang, P.S., Lee, C.K., 2012. *In vitro* inhibition of influenza A virus infection by marine microalga-derived sulfated polysaccharide p-KG03. Antiviral Res. 93, 253–259.
Kuzuhara, T., Iwai, Y., Takahashi, H., Hatakeyama, D., Echigo, N., 2009. Green tea catechins inhibit the endonuclease activity of influenza A virus RNA polymerase. PLoS Curr. 1, RRN1052.
Leneva, I.A., Russell, R.J., Boriskin, Y.S., Hay, A.J., 2009. Characteristics of arbidol-resistant mutants of influenza virus: implications for the mechanism of anti-influenza action of arbidol. Antiviral Res. 81, 132–140.
Li, S., Hattori, T., Kodama, E.N., 2011. Epigallocatechin gallate inhibits the HIV reverse transcription step. Antivir. Chem. Chemother. 21, 239–243.
Lyu, S.Y., Rhim, J.Y., Park, W.B., 2005. Antiherpetic activities of flavonoids against herpes simplex virus type 1 (HSV-1) and type 2 (HSV-2) *in vitro*. Arch. Pharm. Res. 28, 1293–1301.
Matlin, K.S., Reggio, H., Helenius, A., Simons, K., 1981. Infectious entry pathway of influenza virus in a canine kidney cell line. J. Cell Biol. 91, 601–613.
McKimm-Breschkin, J.L., 2013. Influenza neuraminidase inhibitors: antiviral action and mechanisms of resistance. Influenza Other Respir. Viruses 7 (Suppl. 1), 25–36.
Nakayama, M., Suzuki, K., Toda, M., Okubo, S., Hara, Y., Shimamura, T., 1993. Inhibition of the infectivity of influenza virus by tea polyphenols. Antiviral Res. 21, 289–299.

Ohuchi, M., Asaoka, N., Sakai, T., Ohuchi, R., 2006. Roles of neuraminidase in the initial stage of influenza virus infection. Microbes Infect. 8, 1287–1293.
Pleschka, S., Jaskunas, R., Engelhardt, O.G., Zurcher, T., Palese, P., Garcia-Sastre, A., 1996. A plasmid-based reverse genetics system for influenza A virus. J. Virol. 70, 4188–4192.
Schols, D., Pauwels, R., Vanlangendonck, F., Balzarini, J., De Clercq, E., 1988. A highly reliable, sensitive, flow cytometric/fluorometric assay for the evaluation of the anti-HIV activity of antiviral compounds in MT-4 cells. J. Immunol. Methods 114, 27–32.
Song, J.M., Lee, K.H., Seong, B.L., 2005. Antiviral effect of catechins in green tea on influenza virus. Antiviral Res. 68, 66–74.
Song, J.M., Park, K.D., Lee, K.H., Byun, Y.H., Park, J.H., Kim, S.H., Kim, J.H., Seong, B.L., 2007. Biological evaluation of anti-influenza viral activity of semi-synthetic catechin derivatives. Antiviral Res. 76, 178–185.
Sun, Y., Hung, W.C., Chen, F.Y., Lee, C.C., Huang, H.W., 2009. Interaction of tea catechin (−)-epigallocatechin gallate with lipid bilayers. Biophys. J. 96, 1026–1035.
van der Vries, E., Stelma, F.F., Boucher, C.A., 2010. Emergence of a multidrug-resistant pandemic influenza A (H1N1) virus. N. Engl. J. Med. 363, 1381–1382.
Wolkerstorfer, A., Kurz, H., Bachhofner, N., Szolar, O.H., 2009. Glycyrrhizin inhibits influenza A virus uptake into the cell. Antiviral Res. 83, 171–178.
Yang, C.S., Maliakal, P., Meng, X., 2002. Inhibition of carcinogenesis by tea. Annu. Rev. Pharmacol. Toxicol. 42, 25–54.
Yim, J.H., Kim, S.J., Ahn, S.H., Lee, H.K., 2003. Optimal conditions for the production of sulfated polysaccharide by marine microalga Gyrodinium impudicum strain KG03. Biomol. Eng. 20, 273–280.